International Journal of Applied Engineering Research ISSN 0973-4562 Volume 14, Number 6 (2019) pp. 1244-1254
© Research India Publications. http://www.ripublication.com

CPW fed Apollonian Gasket Fractal antenna loaded with Tri-mode ERR for Multiband Operations

Jayarenjini N[a, b], Unni C[b]

[a] *Department of ECE, ACE College of Engineering, Thiruvananthapuram, Kerala 695027, India.*

[b] *LBS Centre for Science and Technology, Thiruvananthapuram, Kerala 695033, India.*

Abstract:

A CPW-fed Apollonian Gasket Fractal (AGF) antenna loaded with Tri-mode Electric Ring Resonator [TERR] for multiple frequency band application is demonstrated in this paper. The design of AGF is done on FR4 glass epoxy substrate which has thickness of 1.6 mm and relative permittivity of 4.4. Different iterations of AGF are performed to improve performance parameters such as radiation pattern, Return Losses (RL), VSWR, Gain (G), etc. The CPW-Fed antenna consists of Tri-mode Electric Ring Resonator [TERR] which is fixed on reverse side of the substrate and iterated AGF is stamped on top of the FR4. Multi band can be obtained by placing a TERR beneath the CPW structure of the antenna. By properly changing the dimensions of the ERR structure, each of the resonating frequency band can be easily tuned. The numerical results show that the proposed antenna has good impedance bandwidth and radiation characteristics in the operating bands at 2.91/6.03/8.09/11.35/15.87 GHz bands which cover up the frequency spectrum of WiFi (IEEE 802.11n), IEEE 802.16e, X-band uplink, S/C/X and Ku band with return loss of better than 10 dB.

Keywords: Fractals, Gasket fractals, Electric Ring Resonators, CPW Feed, WiFi, WLAN.

1. INTRODUCTION

Most modern communication require systems capable of operating in multiple bands and requires antenna with small size, light weight, low profile and can be easily integrated with other microwave components. Most of the applications use the lower end of the UHF band while WLAN and UWB operate in the upper UHF band. Planar antennas with CPW (coplanar waveguide) feed have received much attention due to its wideband characteristics and ease of integration with MMICs [1]-[3]. Fractal antennas are commonly employed to develop multiband antennas because of its inherent properties like small size, self-similarity and multiband capability [4]-[6].

An Apollonian gasket or Apollonian net is a fractal generated starting from a triple of circles, each tangent to the other two, and successively filling in more circles, each tangent to another three. It is named after Greek mathematician Apollonius of Perga. Due to the inherent geometrical ability for wideband matching for impedance, a circular-shaped monopole antenna is chosen so that it can operate over a very wide band. By altering the radiating strip/ground flat and by utilizing dissimilar shapes, multiple band resonating modes can be achieved.

To decrease the complexity and miniaturize antenna dimension, the combination of fractal concept and meta-materials confines the applications of the antenna. Metamaterial are artificial homogeneous structure synthesized to display simultaneously negative permeability and negative permittivity. Split Ring Resonator (SRR) is one of the main elements of metamaterial [8]. Negative permeability characteristics can be achieved by the use of SRR and it can be used for bandwidth improvement. Different SRR structures are reported in the literature such as Multiple Split Ring Resonator (MSRR), Labyrinth Resonator (LR), Spiral Resonator (SR), Broad Side Coupled Split Ring Resonator (BCSRR), and Non-Bianisotropic Split Ring Resonator (NBSRR) [9, 10]. Because of the resonant nature, the design of compact radiating element for CPW-fed antennas and microstrip planar antennas can be employed by SRR.

In this article, Apollonian Gasket Fractal (AGF) patch (Top Side) and Tri-mode Electric Ring Resonator [TERR] (Flipside) antenna are projected for S band/Non-coherent UWB - 2 to 4 GHz, WiFi (IEEE 802.11n) - 2 to 5 GHz, X-band uplink - 8.02 to 8.5 GHz, Ku band downlink -10.7-12.75 GHz, Ku band- 12.5 to 18 GHz. CPW feed is used with source and symmetry ground. The TERR resonance frequency with permittivity characteristics is also studied. The radiation characteristics of the antenna such as S_{11}, Gain, VSWR and impedance bandwidth is mandatory and it is depend on the entire operating frequency. The proposed antenna is designed, simulated and optimized by using electromagnetic simulator software CST microwave studio.

2. ANTENNA DESIGN AND SIMULATED RESULTS

2.1 Antenna Geometry

A CPW fed Apollonian Gasket Fractal (AGF) patch configuration (top view) and Tri-mode Electric Ring Resonator [TERR] (Reverse view) as publicized in the Figure. 1(a) and (b). The antenna is etched on FR-4 substrate having relative permittivity (ε_r) of 4.4, loss tangent ($\tan\delta$) of 0.02 and a thickness of 1.6 mm. The overall dimension of substrate is 30 mm x 30 mm x 1.6 mm.

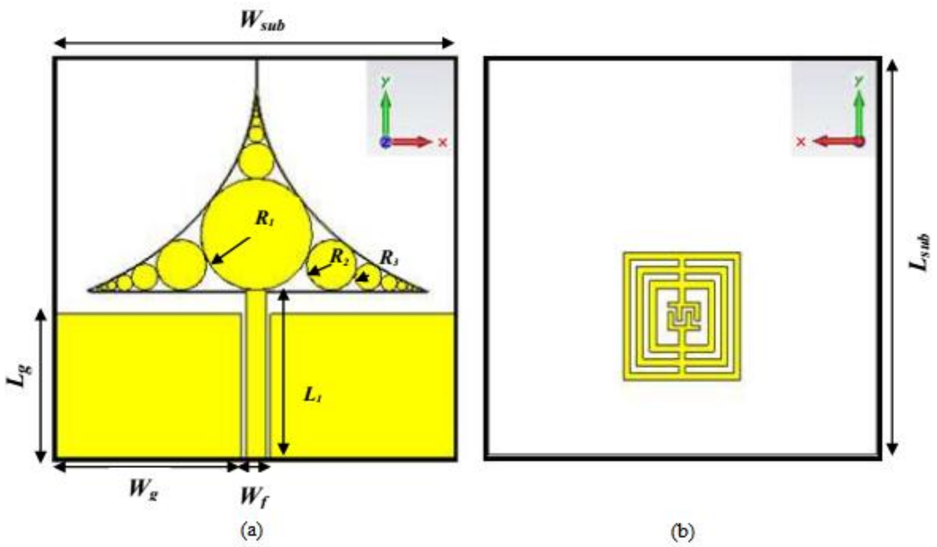

Figure 1. Geometry of CPW Fed Apollonian Gasket Fractal (AGF) patch antenna [Top] and Tri-mode ERR [Bottom].

The antenna is fed by CPW consists of a two symmetry planes and source. The optimized dimensions are listed in Table 1.

Table 1: Optimized Dimensions of the Designed Antenna

Parameters	Dimensions (mm)	Parameters	Dimensions (mm)
$W_{sub}= L_{sub}$	30.0	W_f	1.4
L_1	12.6	R_1	4.0
W_g	13.9	R_2	2.0
L_g	10.8	R_3	1.0

2.2 Design Process

To better explain the antenna design, Figure 2 shows four evolution stages of the antenna. All the parameters of the antenna are optimized stepwise. During the stepwise optimization, one parameter is varied while keeping all other parameters constant, at one time.

The basic or Zeroth iteration of the designed antenna structure consists of two mutually tangent circles and a straight line, coplanar waveguide feeding and partial rectangular ground planes symmetrical to the feed line. Consider mutually tangent circles, and draw their inner Soddy circle. This resulted into first iteration of the antenna structure. In the second iteration, draw the inner Soddy circles of this circle with each pair of the original circles, and continue iteratively.

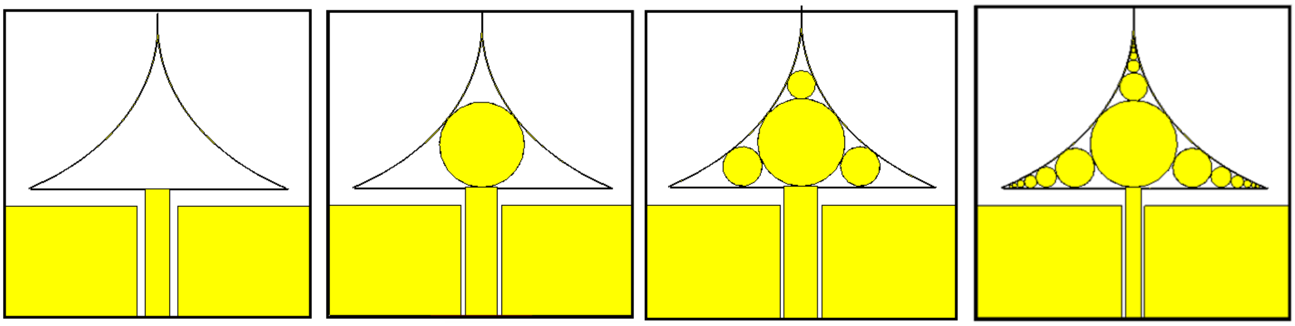

(a) Zeroth Iteration (b) First Iteration (c) Second Iteration (d) Third Iteration

Figure 2. Evolution stages of proposed antenna.

Due to advantages like coplanarity with the radiating patch, wider bandwidth, better impedance matching, lower radiation loss, and less dispersion, the coplanar waveguide feeding technique is used [11]. The comparison of intermediated stages in terms of their reflection coefficient characteristics is shown in Figure 3 and is listed in Table 2. It is observed that as the number of iterations increase from Zeroth to second, the impedance matching is improved. From Zeroth iteration to third iteration, the structures possess dual band characteristics with better impedance matching.

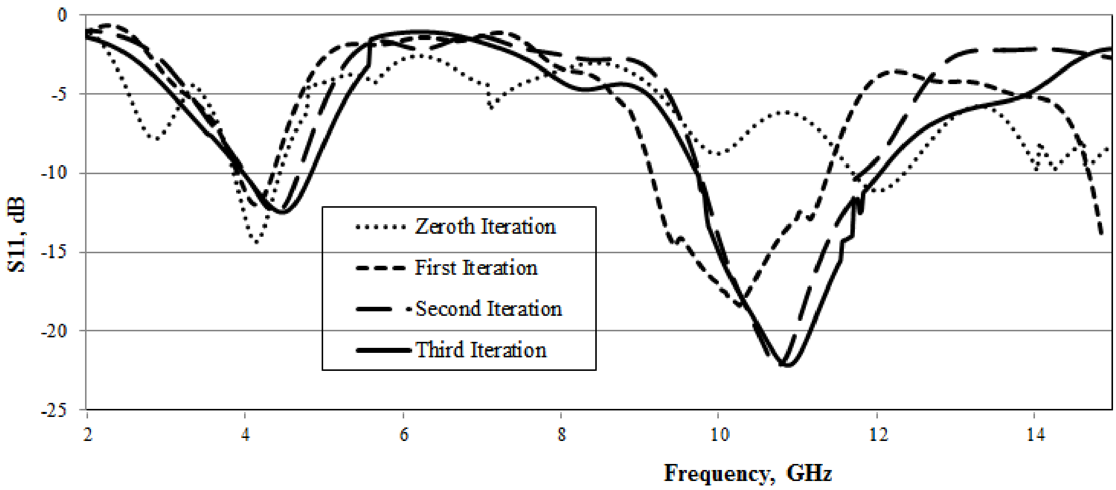

Figure 3. Simulated Reflection coefficient versus frequency characteristic for return loss S_{11} (dB) of antenna evolution stages.

Table 2: Comparisons of four Iterations of the Designed Antenna

Sl. No.	Iterations	f_L (GHz)	f_H (GHz)	BW (GHz)	f_L (GHz)	f_H (GHz)	BW (GHz)
1	Zeroth	3.89	4.45	0.56	11.73	12.33	0.6
2	First	3.92	4.36	0.44	9.17	11.38	2.21
3	Second	4.02	4.68	0.66	9.77	11.82	2.05
4	Third	3.9	4.81	0.91	9.74	12.05	2.31

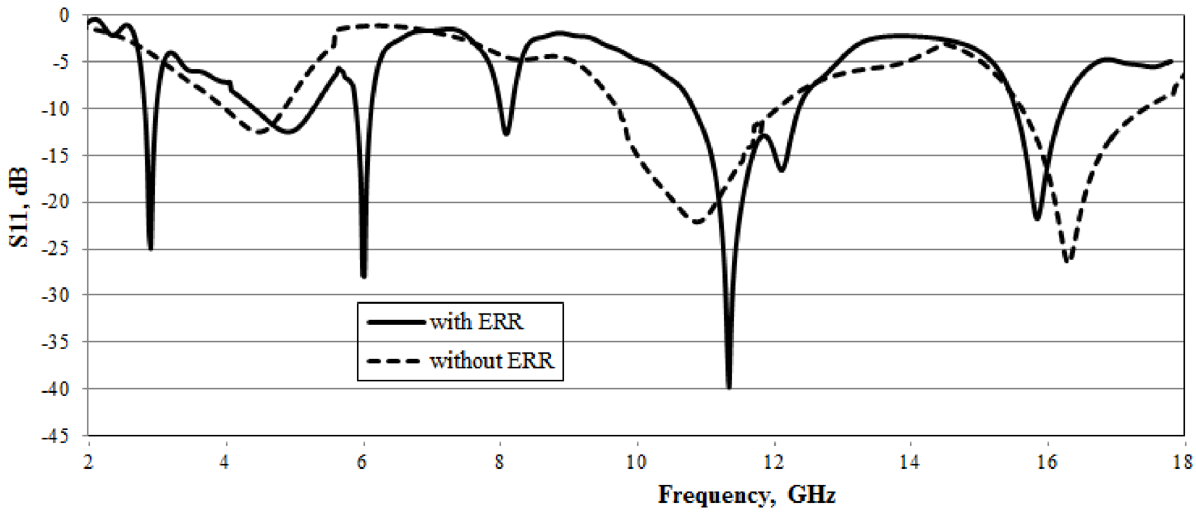

Figure 4. Simulated Return Loss, S_{11} (dB) of antenna loaded with and without TERR.

Figure 4 shows the response of the proposed antenna with and without loading the TERR structure in terms of reflection coefficient. From this result, it is evident that TERR loaded Apollonian Gasket Fractal antenna shows multiband characteristics, in which three resonant frequency bands such as 3.0 GHz, 6.0 GHz and 8.07 GHz are provided by the metamaterial (TERR) structure.

2.3 Parametric Study

The performance of the proposed antenna (as depicted in Figure 1) is affected by certain parameters. In the following research, when one parameter is changed, the others keep the same to analyze the influence. To achieve the design requirements, these parameters provide the designer with more degrees of freedom. The most effective parameters will be examined, and its significance on the antenna response will be assessed. In order to analyze the impact of different parameters of the proposed antenna on return loss, we study the variation of S_{11} with different values of L_1, W_f, and L_g when port 1 was excited.

2.3.1. The effect of height of feed line (L_1)

The effect of the variation on the height L_1 on the antenna performance has been shown in Figure 5, where L_1 has been varied from 12.4 mm to 12.8 mm in steps of 0.2 mm. The location of the lower resonant band and its center frequency are slightly affected. Anyway, the influence on the upper resonant band is more apparent. As the height L_1 increases, the center of the upper resonant band is shifted up and to right, while the corresponding bandwidth becomes wider. Above some specific value of L_1, the upper resonant band starts to weaken.

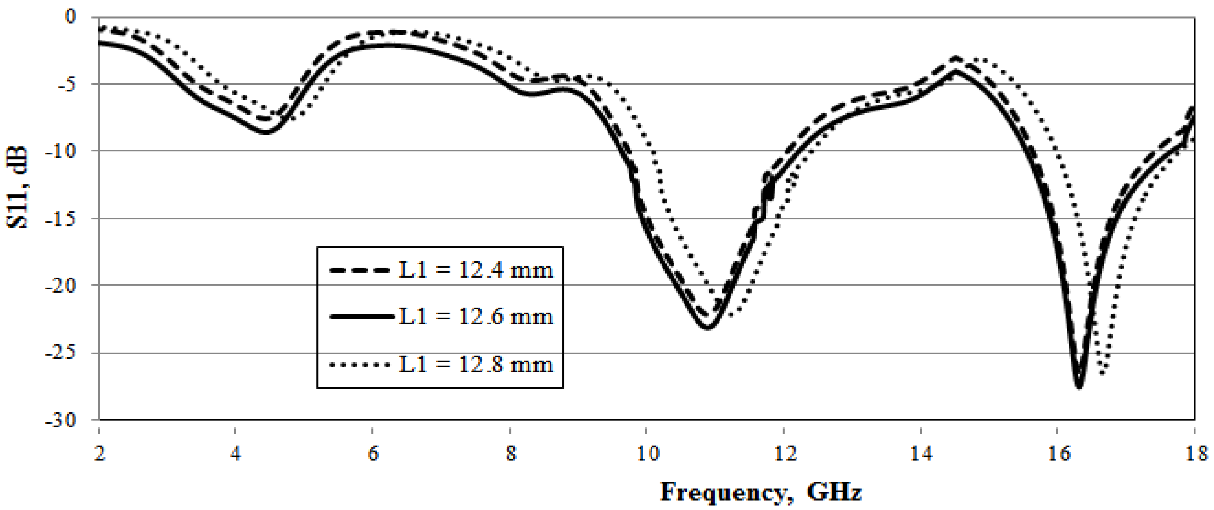

Figure 5. Variation of S_{11}, with feed length L_1.

2.3.2. The effect of width of fedline (W_f)

The effect of the variation of the microstrip feed line width on the antenna performance has been shown in Figure 6, keeping the spacing L_1 and other parameters unchanged, where W_f has been varied from 1.4 mm to 1.6 mm in steps of 0.1 mm. However, the effect on the upper resonant band is more evident. As the width of the feed line increases, the upper resonant band is considerably affected; its position is shifted up while the corresponding bandwidth becomes narrower. Above some certain value of fedline width, the upper resonant band starts to diminish.

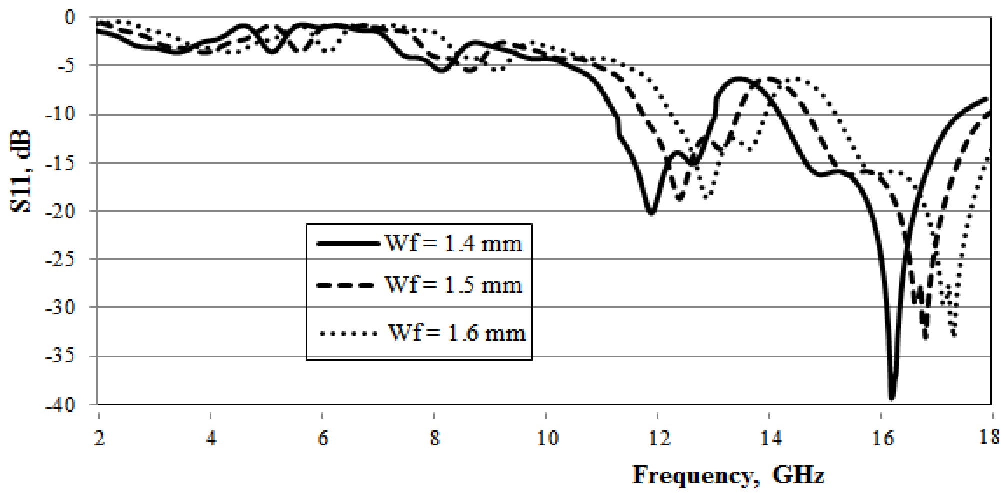

Figure 6. Variation of S_{11}, with different fedline width W_f

2.3.3. The effect of height of ground (L_g)

The effect of the variation of height of ground on the antenna performance has been shown in Figure 7. The antenna ground plane height has been varied from 10.7 mm to 10.9 mm in steps of 0.1 mm. As the height of ground increases, the lower resonant band as well as the upper frequency band is slightly affected; its position is shifted up while the corresponding bandwidth is broadened.

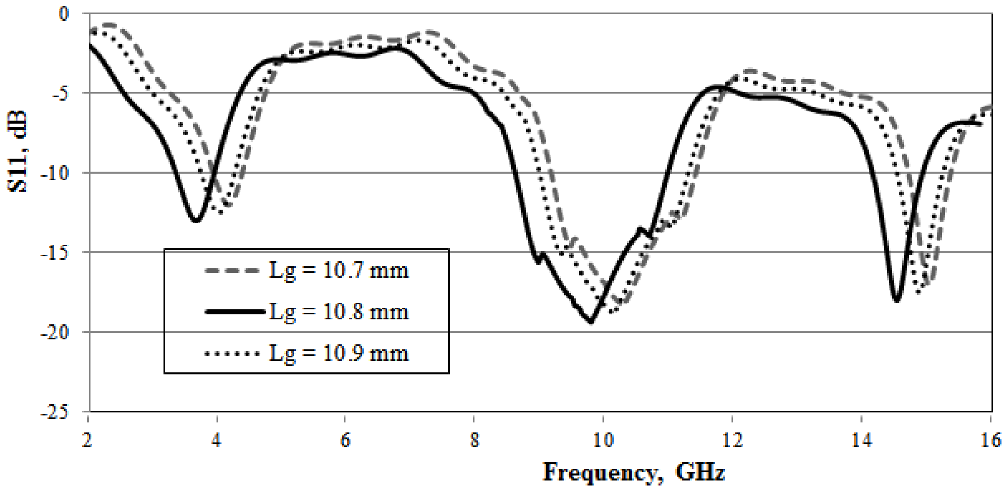

Figure 7. Variation of S_{11}, with different ground height L_g.

2.3.4. Tri-mode Electric Ring Resonator (TERR)

TERR can be used in the design of metamaterial structure [12, 13]. To realize TERR structure and its equivalent circuit, tri-mode structure of the ERR providing a pass band response at the three chosen frequency is used. The frequency of this is controlled by the ERR geometry. Schematic diagram of the ERR consists of a square ring with the quasi-lumped capacitance inside.

The equivalent diagram of the ERR corresponds to a parallel LC-tank [12]. The resonant frequency depends on the inductance L (ring dimensions) and on the capacitance C (the central gap width *Gc* and length *Lc*).

The modified structure of the dual-mode resonator (dual-ERR) consists of two nested square rings. The behavior of the resonances at the first and second frequencies of the dual-ERR has been analyzed during the parametric study of the CPW with dual-ERR [14]. The low-frequency mode is provided by the excitation of the central capacitor and the inner ring. The current in the outer ring is conditioned by a mutual inductance between the rings. This means that, the resonant frequency of the first mode depends on the dimensions of the inner square ring L_1 and the quasi-lumped capacitance *Lc, Gc*. The second mode corresponds to the resonant response of the structure formed by two coupled rings with dimensions L_1 and L_2.

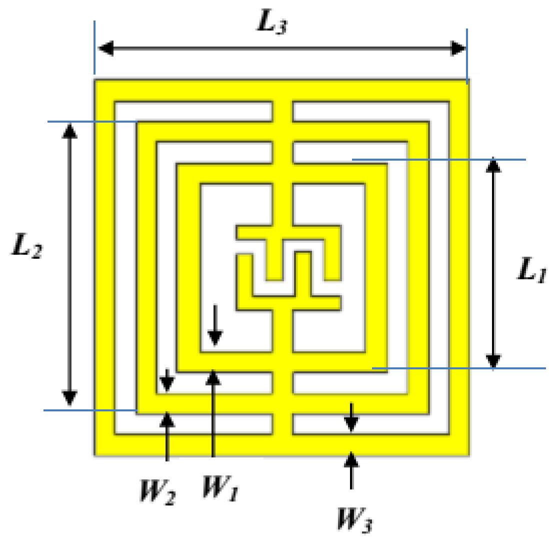

Figure 8. Tri-mode ERR (TERR): Schematic diagram

The tri-mode ERR (tri-ERR) is used for the design of triple band is shown in Figure 8. The tri-ERR (TERR) of the antenna contains three coupled rings and a modified interdigital capacitor. The optimized dimensions are listed in Table 3.

Table 3: Dimensions of the TERR

Parameters	Dimensions (mm)	Parameters	Dimensions (mm)
L_1	5	W_1	1
L_2	7	W_2	0.5
L_3	9	W_3	0.5

The modified interdigital capacitor integrated into the tri-ERR was used for a realization of the first notch at frequency of 3.0 GHz. The low-frequency mode is provided by the excitation of the interdigital capacitor and the inner ring. Two other modes arise from the resonances of structures formed by coupled rings with dimensions L_1, L_2, and L_3. Thus, the triple band antenna design starts with the setting of the first mode by proper choosing the geometry of the capacitance and the inner ring (L_1); then, the third mode is setting by choosing the proper dimension of the middle ring (L_2); and finally, the second mode is setting by choosing the proper dimension of the outer ring (L_3).

In this paper, the Nicolson Ross Wier process is measured to attain the negative permeability of the proposed TERR. The proposed TERR structure is validated with the negative permeability characteristics, waveguide method are worn to describe. The proposed multi-mode Electric Ring structure is placed within waveguide as open in the Figure 9 (a). The TERR loaded Sierpinski square fractal antenna design has exposed notch in the S_{11} characteristics. The real parts of permeability are extracted as given away in Figure 9 (b). Thus the meta-material property proved the effective material constraints.

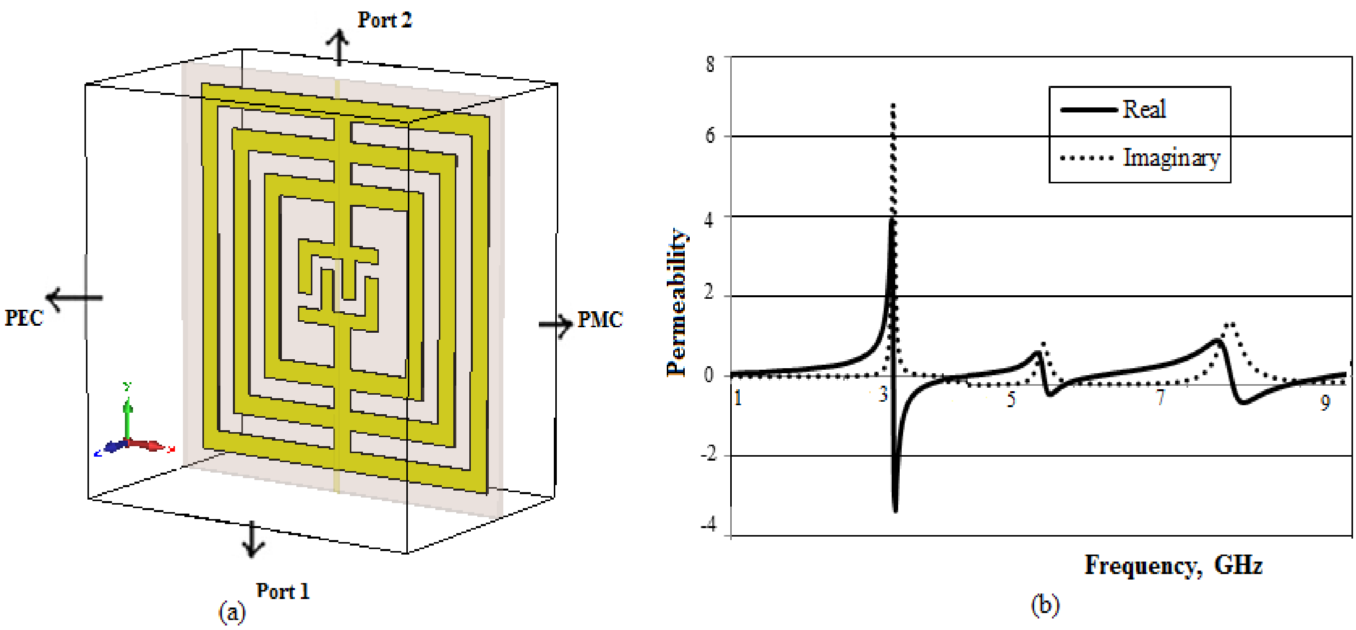

Figure 9. Waveguide Setup for Tri-mode ERR (TERR)

3. RESULTS AND DISCUSSIONS

3.1 Simulation Results

The simulated results show multiple band operations of the proposed fractal antenna which ranges 2.91/6.03/8.09/11.35/15.87 GHz with VSWR is at 1.12/1.09/1.5/1.02/1.13 which covers S/C/X/Ku band, which is useful for applications such as WiFi (IEEE 802.11n), IEEE 802.16e and X-band uplink. To categorize with the behaviour of the antennas reverberating method exciting current distributions of the antenna model are shown in the Figure 10.

For S band frequency, 2 GHz, current is practically in the feed line as revealed in Figure 10 (a). For the 3 GHz, C band is in the iterated Apollonian Gasket Fractal and the maximum current density is in TERR as shown in the Figure 10 (b). For X band frequency 12 GHz, current density in the edging of the iterated Apollonian Gasket Fractal. The simulated gain of the TERR loaded Apollonian Gasket Fractal antenna has 2.22 dBi, 5.35 dBi, 3.83 dBi, 7.08 dBi and 5.50 dBi at center frequencies 2 GHz, 3 GHz, 6 GHz, 8 GHz and 12 GHz respectively. The Simulated gain in 3D Pattern is shown in the Figure 11.

Since Table 4, we can finish that the planned antenna produces superior performance in antenna proportions furthermore covering functional bands than the existing literatures.

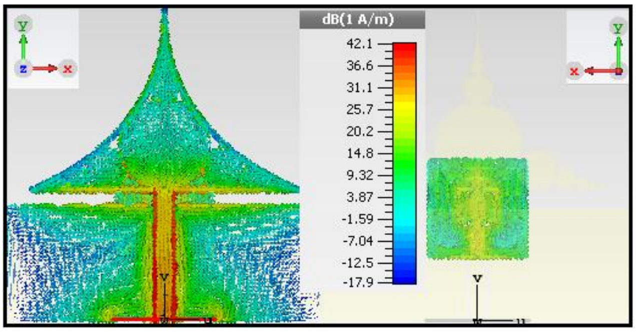

(a) 2 GHz

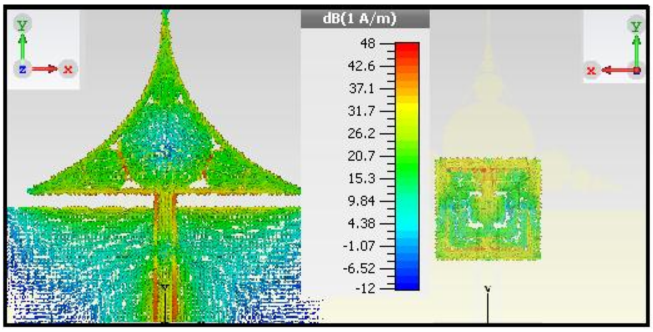

(b) 6 GHz

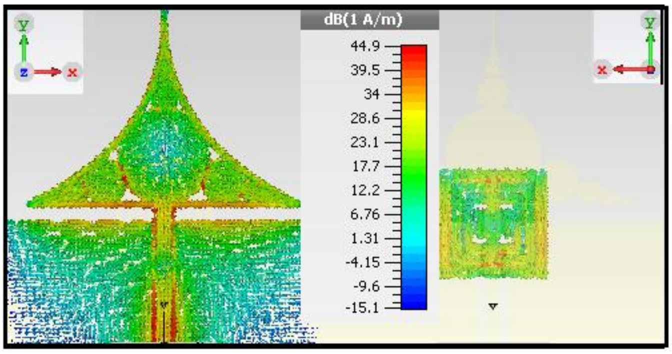

(c) 12 GHz

Figure 10. Simulated surface current distributions for the antenna projected

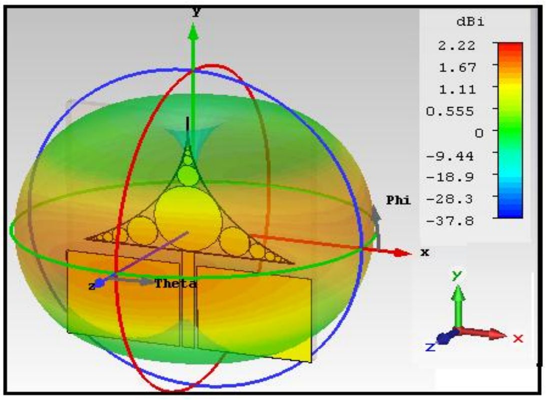

(a) 2 GHz

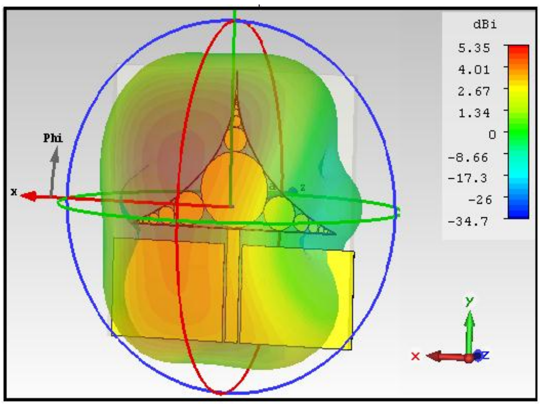

(b) 3 GHz

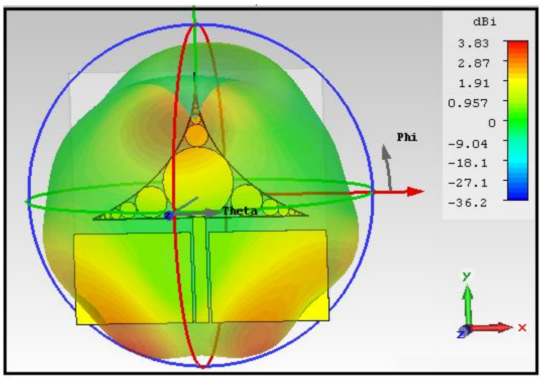

(c) 6 GHz

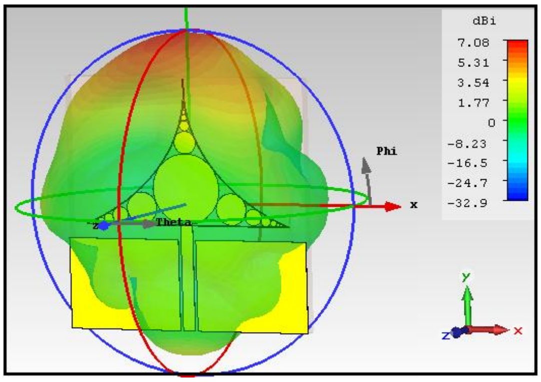

(d) 8 GHz

Figure 11. Simulated Gain in 3D pattern

Table 4: Comparison of different existing fractal MM antennas by way of antenna proposed

Sl. No.	References	Antenna Size (mm^2)	Frequency enclosed (GHz)	Antenna Nature
1	Proposed	30 x 30	2.91/6.03/8.09/11.35/15.87	Muti-band
2	[17]	14 x 16	3.8/8.68	Dual band
3	[16]	32 x 36	1.14/11.8	Dual band
4	[15]	24.3 x 30.8	3.85/4.0	Dual wide band
5	[19]	31.7 x 27	2.65/4.24	Dual band

3.2 Experimental Results

In order to verify the simulated results, Apollonian Gasket Fractal patch configuration (top view) and Tri-mode Electric Ring Resonator [TERR] is fabricated, measured, and compared. Figures 12 (a) and 12 (b) show the fabricated antenna with the TERR on the reverse side.

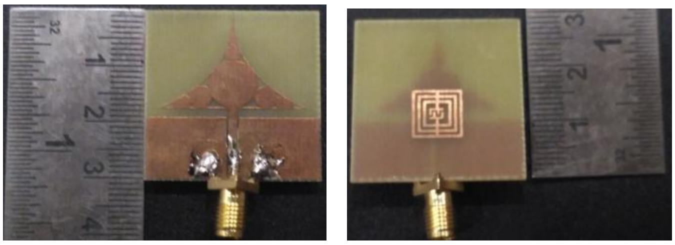

(a) Top view (b) Flipside view.

Figure 12. Snap of the Fabricated TERR loaded Apollonian Gasket Fractal antenna

The measured results show superior agreement of multiple band operations of the TERR loaded Apollonian Gasket Fractal antenna which ranges 2.91/6.03/8.09/11.35/15.87 GHz which covers S/C/Ku band which is useful for WLAN/IEEE 802.16/Wi-MAX applications as exposed in the Figure 13. The return loss characteristic is measured by using vector network analyzer. The simulated/measured antenna parameters are made known in the Table 5.

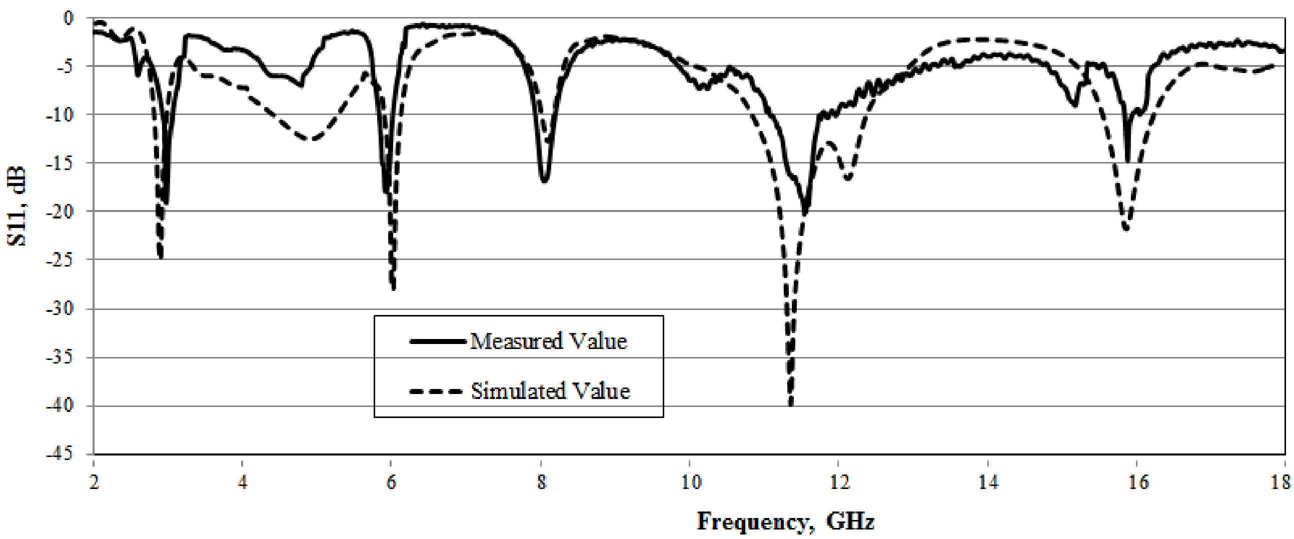

Figure 13. Compared simulated and Measured S_{11}

It is observed that the simulation and experimental results are in good agreement. The discrepancies between the simulation and experimental results can be attributed to the manufacturing tolerances, quality of the SMA connector, and scattering measurement environment. It has resonances at frequencies of 2.91/6.03/8.09/11.35/15.87 GHz which covers S/C/Ku band.

The simulated and measured far-field radiation patterns in E- and H-planes of the antenna at the resonant frequencies of 2.0 GHz, 6.0 GHz, and 8.02 GHz are shown in Figures 14 (a), (b) and (c), respectively. The results show that omnidirectional pattern is observed in *H*-plane and bidirectional radiation pattern observed in *E*-plane. The simulated and measured gains at the resonance frequencies are plotted in Figure 15. The proposed antenna has radiation efficiencies of 50.56%, 97.27%, 91.19%, 96.98% and 93.22% at the resonance frequencies of 2.0 GHz, 3.0 GHz, 6.0 GHz, 8.0 GHz and 12.0 GHz, respectively.

Table 5: Simulated and measured parameters.

Sl. No.	Frequency (GHz)		Reflection Coefficient (dB)		Band Width (GHz)	
	SV	MV	SV	MV	SV	MV
1	2.91	2.98	-24.87	-18.8	170 MHz (2.99-2.82 GHz)	140 MHz (3.07-2.93 GHz)
2	6.03	5.98	-27.95	-17.25	240 MHz (6.14-5.9 GHz)	195 MHz (6..03-5.83 GHz)
3	8.09	8.02	-12.7	-16.27	160 MHz (8.17-8.01 GHz)	280 MHz (8.21-7.93 GHz)
4	11.35	11.56	-39.83	-19.94	1.54 GHz (12.38-10.84 GHz)	690 MHz (11.77-11.08 GHz)
5	15.87	16.0	-21.73	-15.82	680 MHz (16.22-15.54 GHz)	100 MHz (15.93-15.83 GHz)

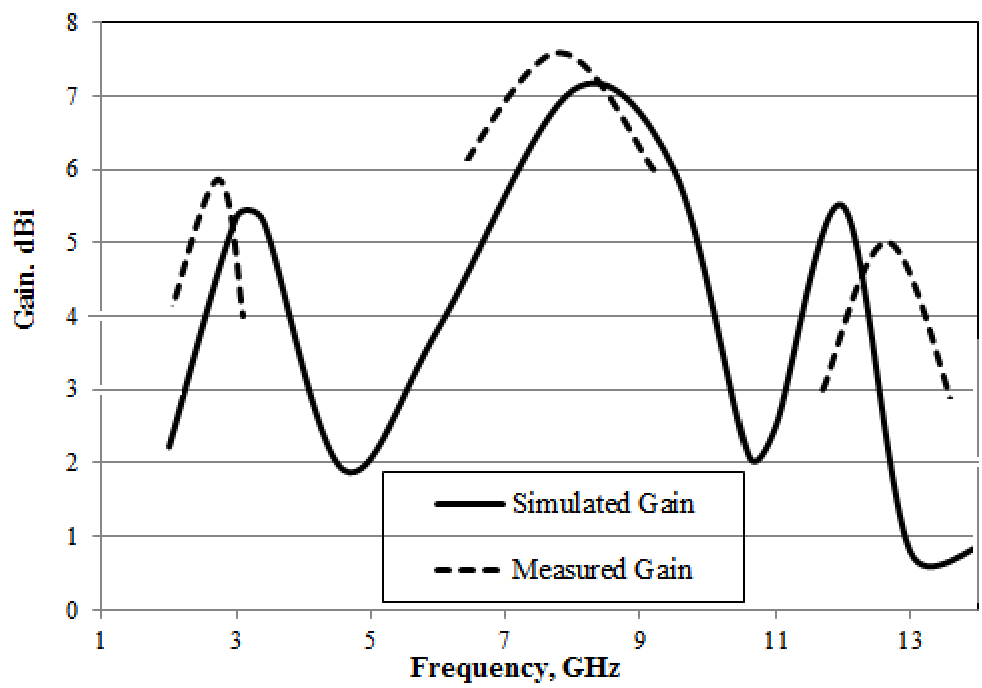

Figure 15. Gain (dBi) of the proposed design over frequency

© Research India Publications. http://www.ripublication.com

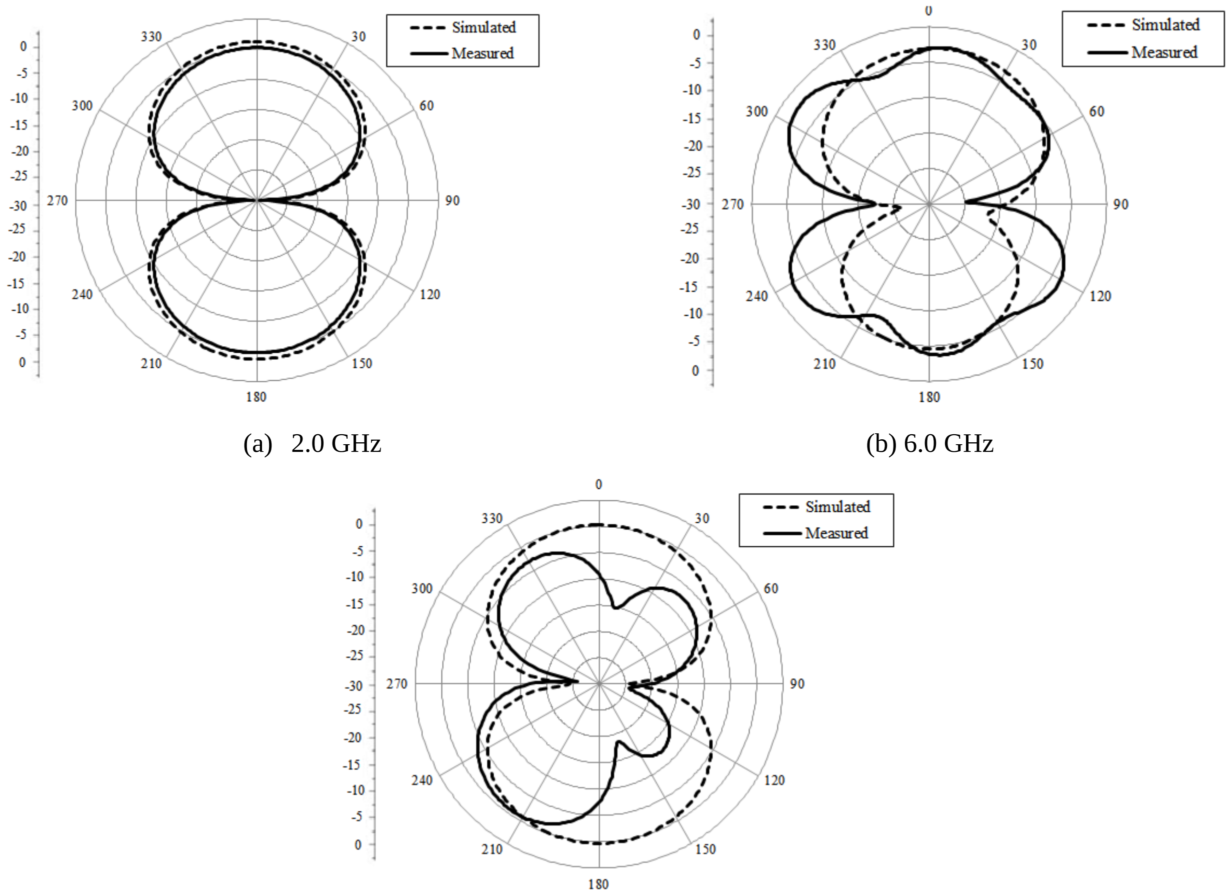

(a) 2.0 GHz (b) 6.0 GHz

(c) 8.02 GHz

Figure 14. Radiation pattern in *E*-plane of proposed antenna at (a) 2.0 GHz. (b) 6.0 GHz. (c) 8.02 GHz.

4. CONCLUSION

A compact Tri-mode Electric ring resonator [TERR] loaded Apollonian Gasket Fractal (AGF) antenna for multiple frequency band operation has been investigated and thoroughly analyzed in this paper. The proposed antenna size reduction has been carried out on the radiating antenna element. The conducted parametric study reveals that the antenna will have an exciting performance making it suitable for integration of many of the recently available communication services. A prototype of the proposed antenna is fabricated and tested. Measured results reveal that the antenna offers multiple resonant bands at 2.91/6.03/8.09/11.35/15.87 GHz bands which cover up the frequency spectrum of WiFi (IEEE 802.11n), IEEE 802.16e, X-band uplink, S/C/X and Ku band. These multiple band antennas can be smoothly integrated by the printed circuit boards (PCBs) of wireless Communication devices.

ACKNOWLEDGMENT

The authors would like to thank Dr. C.K. Anandan, H.O.D, Department of Electronics, Cochin University of Science and Technology, Kerala, India for carrying out measurements.

REFERENCES

[1] Nguyen, D. T., Dong, H. L., Hyun, C. P. Small planar coplanar waveguide-fed dual band-notched monopole ultra wideband antenna. Microwave and Optical Technology Letters, 2011, vol. 53, no. 4, p. 920 - 924.

[2] Yu F., Wang, C. A CPW-Fed novel planar ultra wideband antenna with a band notch characteristic. Radio engineering, 2009, vol. 18, no. 4, p. 551 - 555.

[3] Evangelos, S. A., Argiris, Z. A., Dimitra , I. K., Antonis, A. A., Fotis, L., Kostas, D. Circular and elliptical CPW-fed slot and microstrip-fed antennas for ultrawideband applications. IEEE Antennas and Wireless Propagation Letters, 2006, vol. 5, no. 1, p. 294 - 297.

[4] Mahattanajatuphat , C., Saleekaw, S., Akkaraekthalin, P. A rhombic patch monopole antenna with modified Minkowski fractal geometry for UMTS, WLAN and mobile WIMAX applications. Progress in Electromagnetic Research PIER, 2009, vol. 89, p. 57 - 74.

[5] Gianvittorio, J. P. et al. Fractal antennas: A novel antenna miniaturization technique and applications.

Antenna and Propagation Magazine, 2002, vol. 44, p. 20 - 36.

[6] Azari, A. A new super wideband fractal microstrip antenna. IEEE transactions on Antenna and Propagation, Vol. 59, No. 5, May 2011.

[7] Puente, C., Romeu, J., Pous, R., Cardama, A. On the behavior of the Sierpinski multiband fractal antenna. IEEE Transactions on Antennas and Propagation, 1998, vol. 46, no. 4, p. 517 - 524.

[8] Payam Beigi, Pejman Mohammadi, A novel small triple-band monopole antenna with crinkle fractal-structure, Int. J. Electron. Commun. 70 (2016) 1382–1387 (Elsevier AEU).

[9] Baena, J. D., J. Bonache, F. Martin, R. M. Sillero, F. Falcone, T. Lopetegi, M. A. G. Laso, J. Garcfa-Farcfa, I. Gil, M. F. Portillo, and M. Sorolla, “Equivalent-circuit models for split-ring resonators and complementary split-ring resonators coupled to planar transmission lines,” IEEE Transac ti ons on M i c rowav e Theory and Tec hni q u e s, Vol. 53, 1451–1461, 2005.

[10] Bilotti, F., A. Tos can o, an d L . Vegn i, “Des ign of s p ir al an d mu ltip le s p lit-r in g r es on ator s f or the realization of m in iatu r ized m etam ater ial sam p les,” IEEE Transactions on Antennas and P ropag ati on, Vol. 55, 2258–2267, 2007.

[11] D.C. Chang, B.H. Zeng, and J.C. Liu, CPW-fed circular fractal slot antenna design for dual-band applications, IEEE Trans Antennas Propag 56 (2008), 3630–3636.

[12] D. Schurig, J. J. Mock, and D. R. Smith, “Electric-field-coupled resonators for negative permittivity metamaterials,” Appl. Phys. Lett., vol. 88, 2006.

[13] W. Withayachumnankul, C. Fumeaux, and D. Abbott, “Near-field interactions in electric inductive–capacitive resonators for metamaterials,” Journal of Physics D: Applied Physics, vol. 45, no. 48, Nov. 2012.

[14] A. Rusakov, I. Vendik, K. Kanjanasit, J. Hong, and D. Filonov, “UltraWideband Antenna with Single- and Dual-Band Notched Characteristics Based on Electric Ring Resonator,” in Proc. Days on Diffraction, St. Petersburg, Russia, Jun. 27 - Jul. 1, 2016, pp. 350–355.

[15] Dawar, P.; Raghava, N.S.; De, A.: Ultra wide band, multi-resonance antenna using Swastika metamaterial. Int. J. Microw. Opt. Technol., 11 (6) (2016), 413–420.

[16] Mishra, R.; Pandey, A.: Asymmetric crescent shaped dual band monopole antenna for UWB and GSM 1800/1900 applications. Int. J. Microw. Opt. Technol., 11 (5) (2016), 356–361.

[17] Thankachan, S.; Chandran, A.A.: SRR loaded UWB monopole antenna with WiMAX and WLAN notch. Int. J. Sci. Eng. Technol. Res., 5 (7) (2016), 2397–2400.

[18] N. Mishra, R.K. Chaudhary, A miniaturized ZOR antenna with enhanced bandwidth for WiMAX applications, Microw. Opt. Tech. Lett. 58 (1) (2016) 71–75.

[19] Naser-Moghadasi, M.; Ali Sadeghzadeh, R.; Khajeh Mohammad Lou, R.; Singh Virdee, B.; Aribi, T.: Semi fractal three leaf clover shaped CPW antenna for triple band applications. Int. J. RF Microw. Comput. Aided Eng., 10 (5) (2015), 413–418.

[20] Payam Beigi, Pejman Mohammadi, A novel small triple-band monopole antenna with crinkle fractal-structure, Int. J. Electron. Commun. 70 (2016) 1382–1387 (Elsevier AEU).